

Figure A.16: This figure shows the **separation** and the **overlap** for the parameter **WIDTH** for **NONE**-weights (Equ. A.65) for different 'core' cleaning levels. The **exponent**  $n$  is coded in **colors**. Blue is  $n = 0.5$ , green is  $n = 1.0$ , pink is  $n = 1.5$  and red is  $n = 2.0$ . Different cleaning algorithms are expressed in different marker styles and line styles. **Circles and continuous line** represent 'classic' cleaning, **triangles and dashed line** is 'island' cleaning and **stars with dotted line** are 'mountain' cleaning. The best separation is obtained with 'island' cleaning, an exponent of 1.5 and a cleaning level of 1.5.

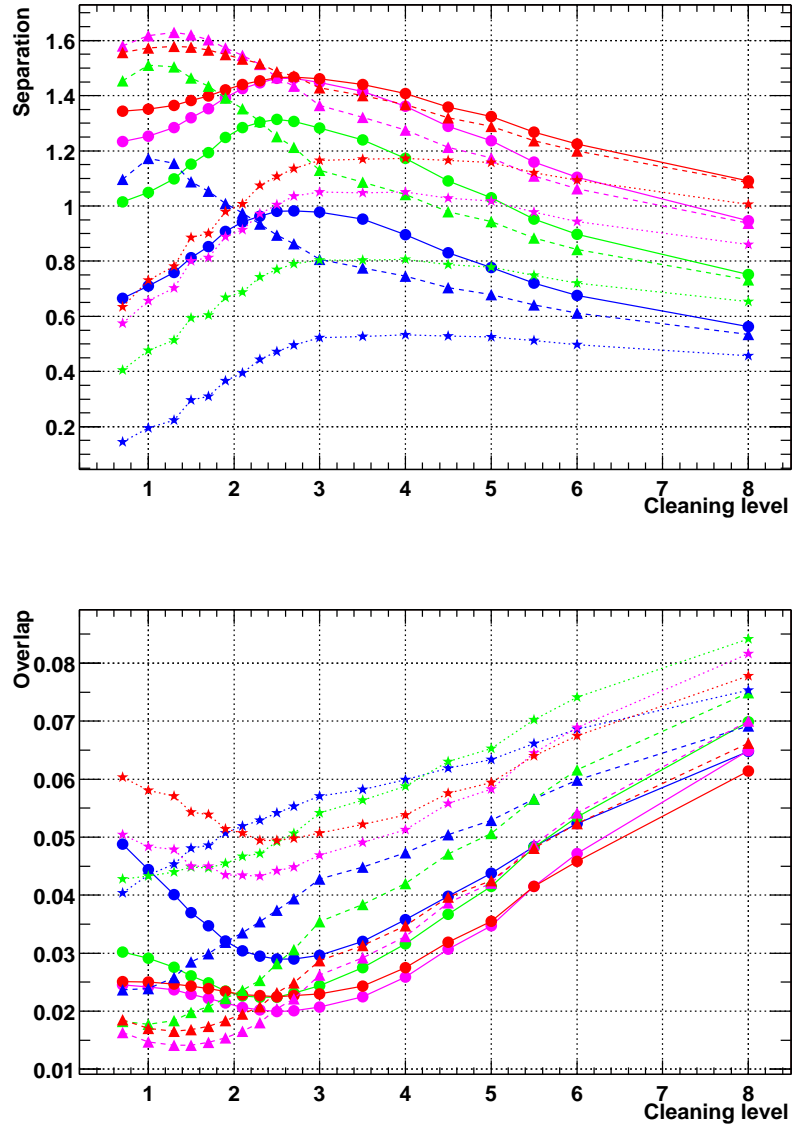


Figure A.17: This figure shows the **separation** and the **overlap** for the parameter **WIDTH** for **REL**-weights (Eq. A.66) for different 'core' cleaning levels. The **exponent**  $n$  is coded in **colors**. Blue is  $n = 0.5$ , green is  $n = 1.0$ , pink is  $n = 1.5$  and red is  $n = 2.0$ . Different cleaning algorithms are expressed in different marker styles and line styles. **Circles and continuous line** represent 'classic' cleaning, **triangles and dashed line** is 'island' cleaning and **stars with dotted line** refer to 'mountain' cleaning. The best separation is obtained with 'island' cleaning, an exponent of 1.5. REL weights give results identical to NONE weights.

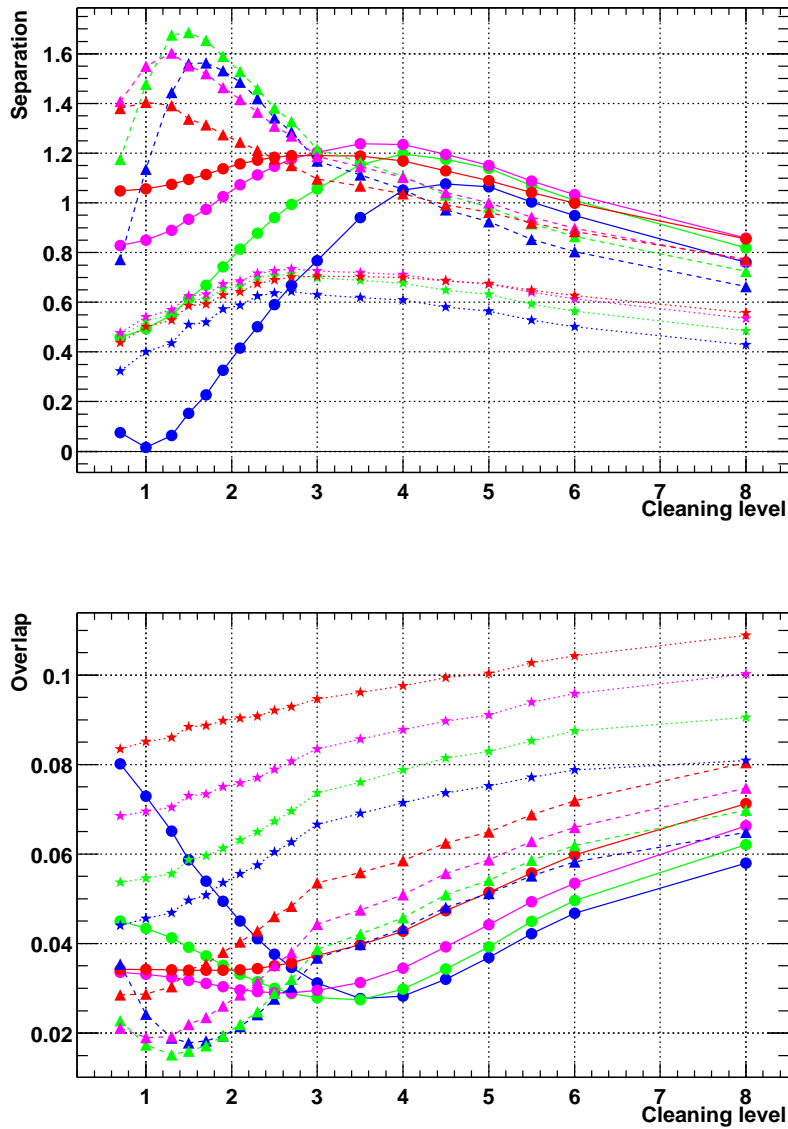


Figure A.18: This figure shows the **separation** and the **overlap** for the parameter **LENGTH** for **NONE**-weights (Equ. A.65) for different 'core' cleaning levels. The **exponent**  $n$  is coded in **colors**. Blue is  $n = 0.5$ , green is  $n = 1.0$ , pink is  $n = 1.5$  and red is  $n = 2.0$ . Different cleaning algorithms are expressed in different marker styles and line styles. **Circles and continuous line** represent 'classic' cleaning, **triangles and dashed line** refer to 'island' cleaning and **stars with dotted line** are 'mountain' cleaning. The best separation is obtained with 'island' cleaning, an exponent of 1.0 and a cleaning level of 1.5.

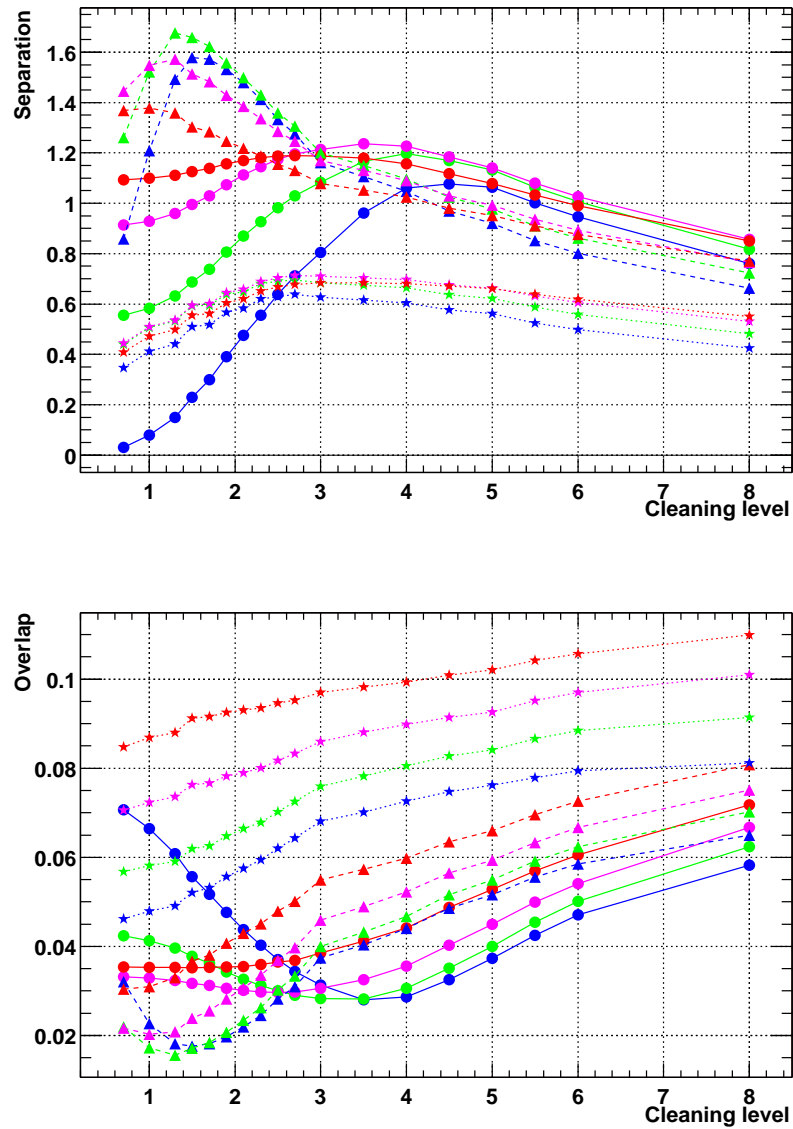


Figure A.19: This figure shows the **separation** and the **overlap** for the parameter **LENGTH** for **REL**-weights (Equ. A.66) for different 'core' cleaning levels. The **exponent**  $n$  is coded in **colors**. Blue is  $n = 0.5$ , green is  $n = 1.0$ , pink is  $n = 1.5$  and red is  $n = 2.0$ . Different cleaning algorithms are expressed in different marker styles and line styles. **Circles and continuous line** represent '**classic**' cleaning, **triangles and dashed line** is '**island**' cleaning and **stars with dotted line** are '**mountain**' cleaning. The best separation is obtained with 'island' cleaning, an exponent of 1.0 and a cleaning level of 1.5. REL-Weights give results identical to NONE-weights.

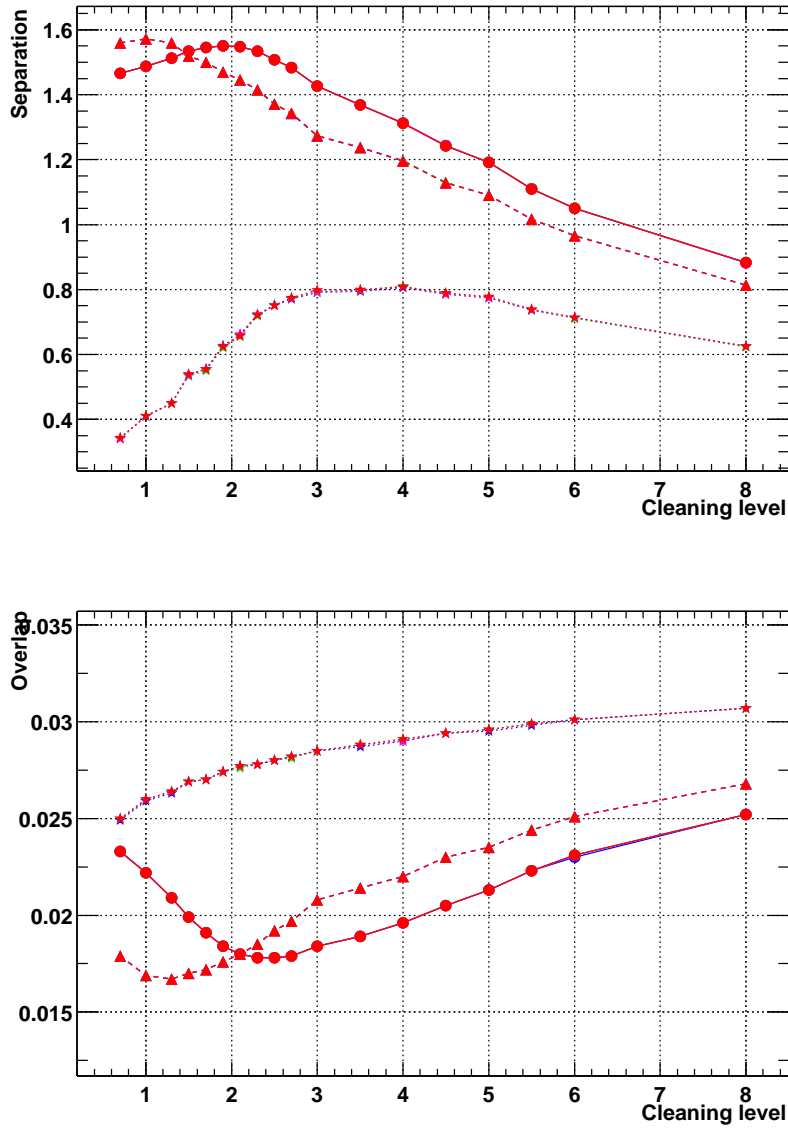


Figure A.20: This figure shows the *separation* and the *overlap* for the parameter *LENGTH* for *NONE*-weights (Equ. A.66) for different 'core' cleaning levels. The *exponent*  $n$  is coded in *colors*. Different cleaning algorithms are expressed in different marker styles and line styles. *Circles and continuous line* represent 'classic' cleaning, *triangles and dashed line* is 'island' cleaning and *stars with dotted line* are 'mountain' cleaning. The best separation is obtained with 'island' cleaning and a cleaning level of 1.0.

Parameter	Cleaning type	Level	Exp.	Sep.	Overlap
WIDTH	'classic'	3.0/2.5	1.0	1.278	0.0238
LENGTH	'classic'	3.0/2.5	1.0	1.057	0.0279
WIDTH	'classic'	2.7/2.0	2.0	1.464	0.0200
<b>WIDTH</b>	<b>'island'</b>	<b>1.3/0.3</b>	<b>1.5</b>	<b>1.630</b>	<b>0.0139</b>
LENGTH	'classic'	3.5/2.7	1.5	1.235	0.0345
<b>LENGTH</b>	<b>'island'</b>	<b>1.3/0.3</b>	<b>1.0</b>	<b>1.676</b>	<b>0.0151</b>
<b>CONC</b>	<b>'island'</b>	<b>1.0/0.3</b>	<b>/</b>	<b>1.584</b>	<b>0.0180</b>

Table A.2: The table shows the **cleaning levels** for the **best** separations and overlaps for WIDTH, LENGTH and CONC for the **two** cleaning algorithms, '**classical**' and '**island**' cleaning. The weights REL and NONE show almost **identical** results (see Fig. A.17, Fig. A.16, Fig. A.18 and Fig. A.19). The first two rows show the old 'classic' version of HILLAS parameters. The cleaning **level** consists of two numbers, the 'image core limit' and the 'image border limit'. 'Exp' denotes the exponent  $n$  and 'Sep' is the separation.

The best cleaning algorithms for WIDTH and LENGTH are printed in bold.

Cleaning type	Level	Exponent	Mean	Variance
'classic'	3.0/2.5	1.0	12.8	11.8
'classic'	3.0/2.5	1.5	10.0	8.4
'classic'	4.0/3.0	1.5	8.4	6.4
<b>'island'</b>	<b>4.0/3.0</b>	<b>1.5</b>	<b>3.9</b>	<b>3.9</b>

Table A.3: The table shows the best conditions to obtain the sharpest ALPHA distribution for point sources. The mean and the variance are the quantities that quantify the sharpness. The first row shows the sharpness of the 'classic' ALPHA as defined by HILLAS. The sharpest ALPHA distribution is obtained by increasing  $n$  to  $n = 1.5$  and by removing the 'islands' with the 'island' cleaning algorithm.

### Conditions to obtain the sharpest ALPHA distribution

The same procedure was applied to analyze the **conditions** to obtain the **sharpest** ALPHA distribution (for  $\gamma$ -events and for point sources). The two **quantities** that characterize the **sharpness** are the **variance** and the **mean** of the ALPHA distribution and they should be kept as **small** as possible. The **smaller** these two the quantities, the **better** the background suppression. Fig. A.21 illustrates both values for different **cleaning levels**, cleaning **algorithms** and different **exponents**  $n$ , as before. The colors and markers are coded in the same way as described above.

A cut of  $0.4 < DIST < 1.05$ ,  $SIZE > 100$  and  $12 \text{ deg} \leq Zenith \text{ angle} \leq 22 \text{ deg}$  was applied beforehand ('precut'). It has to be mentioned that the cut on the zenith angle results in a sharper distribution than the total average has. The conditions for the sharpest ALPHA distribution are listed in Tab. A.3. The very best one is printed in bold.

As a conclusion of these studies we can summarize:

1. Increasing the **exponent**  $n$  to  $n = 1.5$  results in a sharper ALPHA distribution.
2. Increasing the **cleaning level** to **4.0/3.0** also reduces mean and variance of the ALPHA distribution.
3. The **largest** effect is obtained by **removing the islands** from the image before calculating ALPHA.

Unfortunately the miss-pointing of the CT1 telescope is quite large and even after a pointing correction of the recorded data the ALPHA distribution does not have the sharpness that

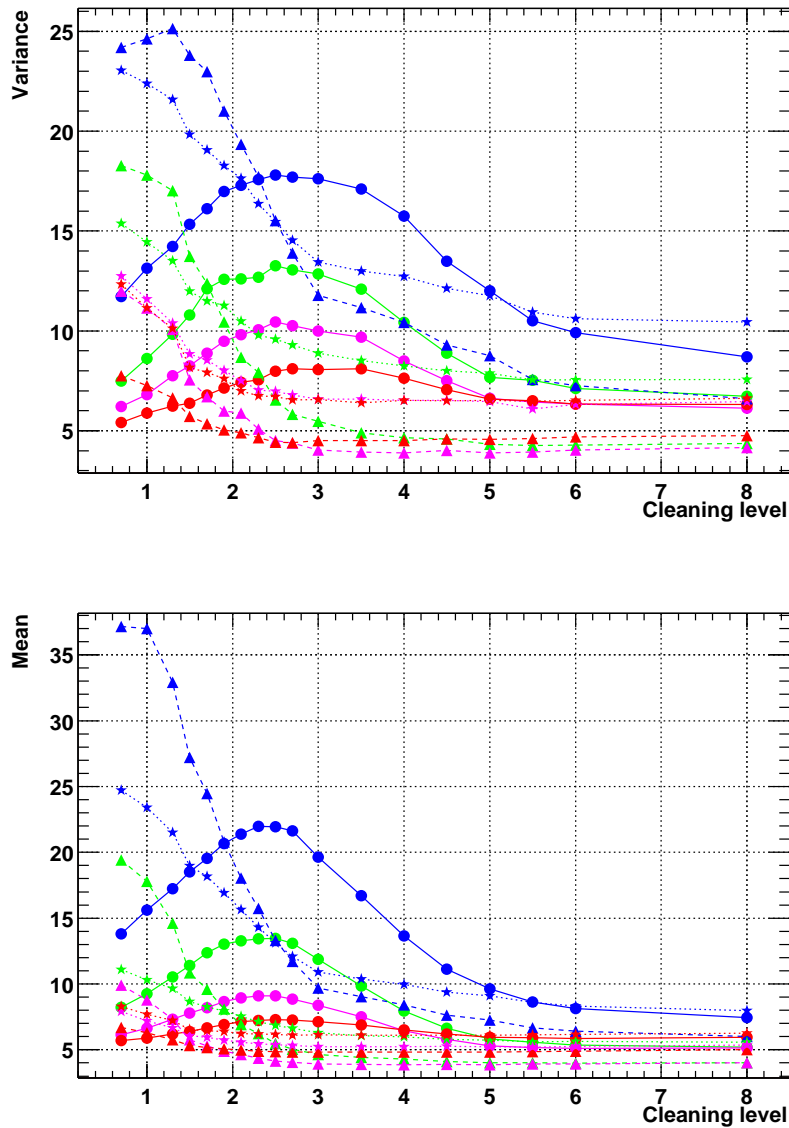


Figure A.21: This plot shows the variance and the mean of the ALPHA distribution of gamma shower images for different 'core' cleaning levels. The smaller these quantities, the better for the background reduction. The exponent  $n$  is coded in colors. Blue is  $n = 0.5$ , green is  $n = 1.0$ , pink is  $n = 1.5$  and red is  $n = 2.0$ . Different cleaning algorithms are expressed in different marker styles and line styles. Circles and continuous line represent classic cleaning, triangles and dashed line is 'island' cleaning and stars with dotted line are 'mountain' cleaning. The sharpest ALPHA distribution is obtained for high cleaning levels above 3 and exponents of 1.5.

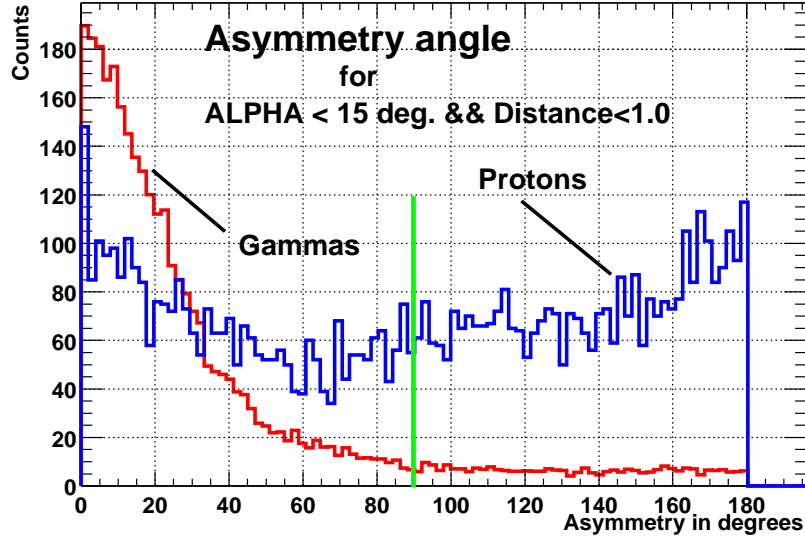


Figure A.22: The asymmetry distribution for gammas and hadrons.  $0^\circ$  points towards the camera center and  $180^\circ$  points away from the camera center. The histogram has been filled **after a cut on ALPHA**  $< 15^\circ$  and  $DIST < 1.0$ . The cut on ALPHA has been performed to demonstrate that only in the case of  $\gamma$ -events the asymmetry is correlated to ALPHA and not for hadronic events. For that reason it is possible to **suppress in the ideal case half of the background** (for a cut on the asymmetry angle at  $90^\circ$ ). The hadron distribution has been scaled up for better visibility.

would be expected from MC studies. We will only be able to take little advantage of the sharper ALPHA distribution.

#### A.4.2 The head-tail asymmetry defined in a such way that it overcomes the finite resolution of the CT1 camera

In the chapter 1, concerning theory and detectors, it was mentioned that all shower images (including hadronic ones) have a **head-tail asymmetry** with respect to the direction from where they originated (Fig. A.22) due to the imaging process which involves a **tangent** of the viewing angle. For point sources this knowledge can be used to **further reduce** the background since the hadronic shower arrive randomly from all directions and the gamma showers only arrive from the center of the camera (if the center points to the source). This idea is not new and has already been used by other experiments. They defined the asymmetry in the following way [Pet97]:

$$\vec{A} = \overline{x_{HP}} - \langle \vec{x} \rangle \quad (\text{A.69})$$

This is the difference between the coordinates of the highest pixel and the shower center of gravity (Equ. A.16). However, this definition has a problem. Since the difference between  $\overline{x_{HP}}$  and  $\langle \vec{x} \rangle$  and the resolution of the CT1 camera ( $0.25^\circ$ ) are of the same order of magnitude doesn't yield good results.

#### The definition of the asymmetry angle

Here I introduce another formalism which uses the **weighted average** of all pixels combined and avoids the pixel size problem. The idea behind this method is the fact that as the **exponent**  $n$  in Equ. A.65 **increases**, the weighted mean (Equ. A.16) moves **in the**



**direction to the shower maximum** and vice versa. Consequently, the **derivative** of the weighted mean with respect to the exponent leads consequently to a vector of **steepest descent** (as seen from the shower maximum) which characterizes an asymmetry in the image.

$$\begin{aligned}\vec{A} &= \left. \frac{d\langle \vec{x} \rangle}{dn} \right|_{n=2} & (A.70) \\ &= n \left[ \frac{(\sum_i q_i^{n-1} \vec{x}) - \langle \vec{x} \rangle \sum_i q_i^{n-1}}{\sum_i q_i^n} \right]\end{aligned}$$

$$\cos \alpha = \frac{\langle \vec{A}, \langle \vec{x} \rangle \rangle}{|\vec{A}| |\langle \vec{x} \rangle|} \quad (A.71)$$

where  $\alpha$  is the angle between the asymmetry vector and the vector from the shower mean to the center of the camera (similar as ALPHA). The parameter  $\alpha$  will be called **asymmetry angle**. The value of the angle  $\alpha$  ranges from 0 to 180°, where 0° points towards the center and 180° points outside of the camera.

In case of  $\gamma$ -events (not in case of hadrons!) ALPHA is strongly **correlated** with the asymmetry angle  $\alpha$ . This formula is still not perfect since many events are truncated at the camera border. With these truncations the asymmetry vector is **no longer** calculated correctly and it points outside of the camera instead of at the center. To avoid this problem, **only** the pixels within a **radius** of  $r = \text{Min}(1.5 - |\vec{x}_{HP}|, 0.25)$  around the **pixel with largest signal** are included in the calculation.

#### Finding the best cleaning conditions and exponents $n$ for the asymmetry

Just as with the other parameters, tests have been performed by **systematically changing** the values and algorithms for image cleaning and the exponents  $n$ . To determine which are the best conditions, another parameter called **cut efficiency** was introduced. It is the ratio of the number of events below 90° (of the asymmetry angle) to the total number of events  $\varepsilon = N(\text{Asymmetry} < 90^\circ) / N_{\text{Tot}}$ .

In Fig. A.23 the **cut efficiency** is plotted for (recorded) **hadronic events** and for MC **gamma events**. As before, circle markers represent 'classic' image cleaning, triangles 'island' image cleaning and stars 'mountain' image cleaning. The colors blue, green, pink and red represent the exponents ( $n=0.5, 1.0, 1.5$  and  $2.0$ ).

As a conclusion it can be stated the following:

1. In case of the asymmetry a **high cleaning level**, just as for the ALPHA distribution, is favored.
2. The best asymmetry distribution results from a **cleaning level** of about **4.0/3.0** using the **'island' cleaning** algorithm and an **exponent** of  $n = 2.0$ .

The resulting distribution can be seen in Fig. A.22. The asymmetry of the hadron distribution originates from events which have been partially truncated at the camera border. A cut of  $0.4 < \text{DIST} < 1.05$ ,  $\text{SIZE} > 100$  and  $12^\circ < \text{zenith angle} < 22^\circ$  was applied beforehand.

#### A.4.3 The problem of truncated images due to the limited size of the CT1 camera and the leakage parameter

As mentioned above, shower images that have large impact parameters or high energies are larger than the camera's field of view so that the image is **truncated** at the camera border. Unfortunately, this occurs for the **majority** of the showers since the number of  $\gamma$  events

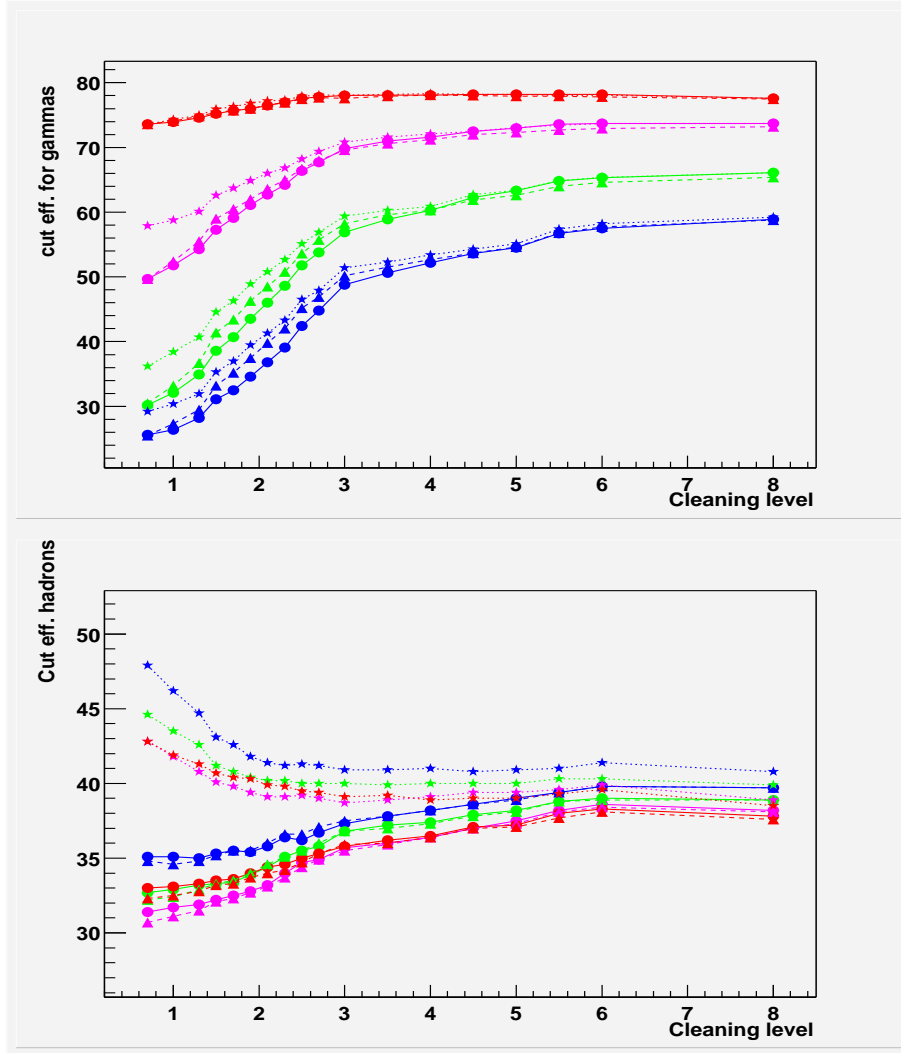


Figure A.23: In this figure the **cut efficiency** of gamma showers (upper plot) and hadronic showers (lower plot) for a cut of  $Asymmetry < 90 \text{ deg}$  is plotted for different 'core' cleaning levels and algorithms. The **exponent**  $n$  is coded in colors. Blue is  $n = 0.5$ , green is  $n = 1.0$ , pink is  $n = 1.5$  and red is  $n = 2.0$ . Different **cleaning algorithms** are expressed in different **marker styles** and **line styles**. **Circles and a continuous line** represent **classic cleaning**, **triangles** and a **dashed line** refer to **'island'** cleaning and **stars with a dotted line** represent **'mountain'** cleaning. The highest hadronic **suppression** (60 %) while retaining most gamma events (78%) is obtained for cleaning levels **above 3** and an **exponent of  $n=2.0$** . The cut efficiency for gammas does never reach 100% since a cut of  $0.4 < DIST < 1.05$ ,  $SIZE > 100$  and  $12^\circ < \text{zenith angle} < 22^\circ$  was applied beforehand.

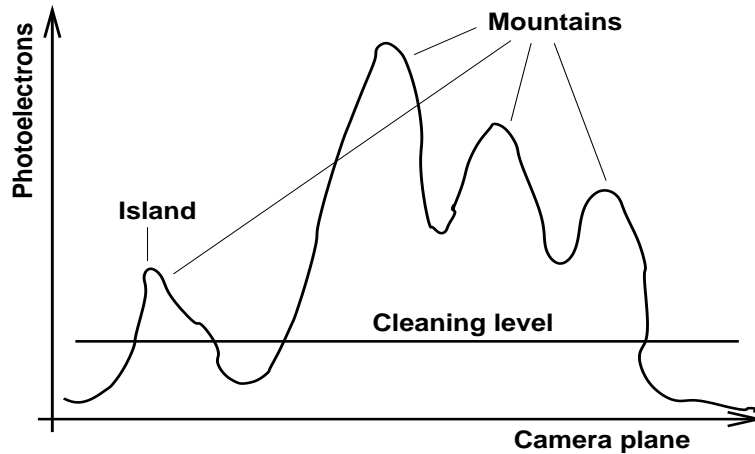


Figure A.24: The figure illustrates what is meant with the expressions '*mountain*' and '*island*'. Islands can form **after** performing a '*classic*' image cleaning of a shower image, depending on the cleaning level. They are isolated clusters that have no connection to other clusters. For simplicity '*islands*' are also called '*mountains*'. In an '*island*' image cleaning only islands are removed. In a '*mountain*' image cleaning all the mountains and islands are **removed** apart of the largest mountain.

increases linearly with the impact parameter. If part of the shower is outside the camera then not all of the light will be collected and measured. This leads to an incorrect energy estimation for showers with large **impact parameters** and high **energy**.

Therefore, a parameter that **quantifies** the truncation is needed. For this purpose, I introduce a simple parameter, called **LEAKAGE**, defined as:

$$LEAKAGE = \frac{\sum_{Border\ pixels} q_i}{SIZE} \quad (A.72)$$

It is the ratio of the charge content of the border pixels and the total charge (i.e. SIZE). In Fig. 1.17 we see the profile of a typical shower. It is clear that by knowing the amplitude at say  $DIST=1.5^\circ$  and also its integral from  $0^\circ$  to  $1.5^\circ$  we can estimate the content of the tail quite well. Later, I will show later that this parameter **increases the resolution of the energy estimation**.

#### A.4.4 Mountains and islands in the shower image: Difference between electromagnetic showers and hadronic showers

The main difference between hadronic showers and electromagnetic showers is the larger **WIDTH** and larger **fluctuations** of hadronic showers. An hadronic shower has a core of high energy hadrons that develop **electromagnetic subshowers**. Seen by a Cherenkov telescope a hadronic shower looks like the **superposition** of several, dispersed, **low energy** electromagnetic showers. As a consequence, the Cherenkov image of a hadronic shower has more '*mountains*' in the sense of Fig. A.24. The electromagnetic shower consists ideally of **one large peak**. I tried to quantify this difference by carrying out a structure analysis, i.e. by **counting** the '*mountains*' in the image.

##### The mountain finding algorithm

I performed a **recursive cluster analysis**, by separating the image into individual clusters. Each cluster contained one mountain. The mountain search method was as follows:

- Perform a '*classic*' image cleaning (without removing islands).

- In a first step, find the **peak pixels** using a recursive algorithm. The peak pixels are the ones that have a **larger** content than all the neighbour pixels. Afterwards **sort** this list, in ascending order.
- Introduce a **cluster object** for each peak pixel.
- Start with the **largest** signal pixel (top) and search recursively **downhill** from the top to the **valley** around the mountain. Put all these pixels, **including** the valley pixels, into the cluster. Treat each pixel only **once** and **mark** those already used. Valley pixels are defined such: There is no unmarked neighbour pixel with lower content.
- Repeat the procedure until all the pixels have been **assigned** to clusters.
- Count the **number of mountains** (-> this is the parameter **Number-Mountain**) and **count the charge** in all the mountains, except from the largest mountain. (-> this is the parameter **Mountain-SIZE**). This parameter quantifies the charge which is **not** inside the largest mountain (for  $\gamma$ -showers ideally zero).

The two new parameters Number-Mountain and Mountain-SIZE give a good estimate of which part of the charge is found in sub-showers. This quantity is very **different** for gamma showers and hadronic showers.

### The island finding algorithm

Before continuing with finding the best **conditions** for these two parameters I want to introduce another algorithm which is used for the **'island' image cleaning**. It is similar to the cluster/mountain analysis and I called it the 'island' analysis. An 'island' is a cluster that is isolated in a cleaned camera. A shower image (after 'classic' cleaning) usually consists of one main island (the main shower image) and some additional islands which are much **smaller**.

The algorithm does the following:

- Perform a **'classic'** image cleaning
- Loop over the pixel list and call a **recursive** algorithm finding the neighbour pixels for each pixel. Continue the recursion with the neighbour pixels. **Mark** each seen neighbour pixel and stop at the **border** of the island. Treat only unmarked pixels. Introduce a **cluster object** for each new unmarked pixel and assign all the pixels of one **island** to this cluster.
- Count the **number of islands** and calculate the **charge** of each island.

The cluster list obtained by the island or mountain analysis can be used for **image cleaning**, leaving only the largest island or mountain. I call these cleaning algorithms **'island'** and **'mountain'** cleaning.

### Gamma/hadron separation

In this work only the mountain analysis is used for gamma/hadron separation purposes. As before, a systematic procedure was used to check the best **conditions** in terms of cleaning level, to provide fore for best separation of gammas and hadrons. The parameters 'separation' and 'overlap' are shown in Fig. A.25 and Fig. A.26.

The results are displayed in Tab. A.4. In these two cases the smallest overlap does not coincide with best separation because of completely non-Gaussian distributions. The value that was chosen as **optimal cleaning level was 3.5/2.7**. (The cleaning level consists of two numbers. A 'core' limit and a 'border' limit.).

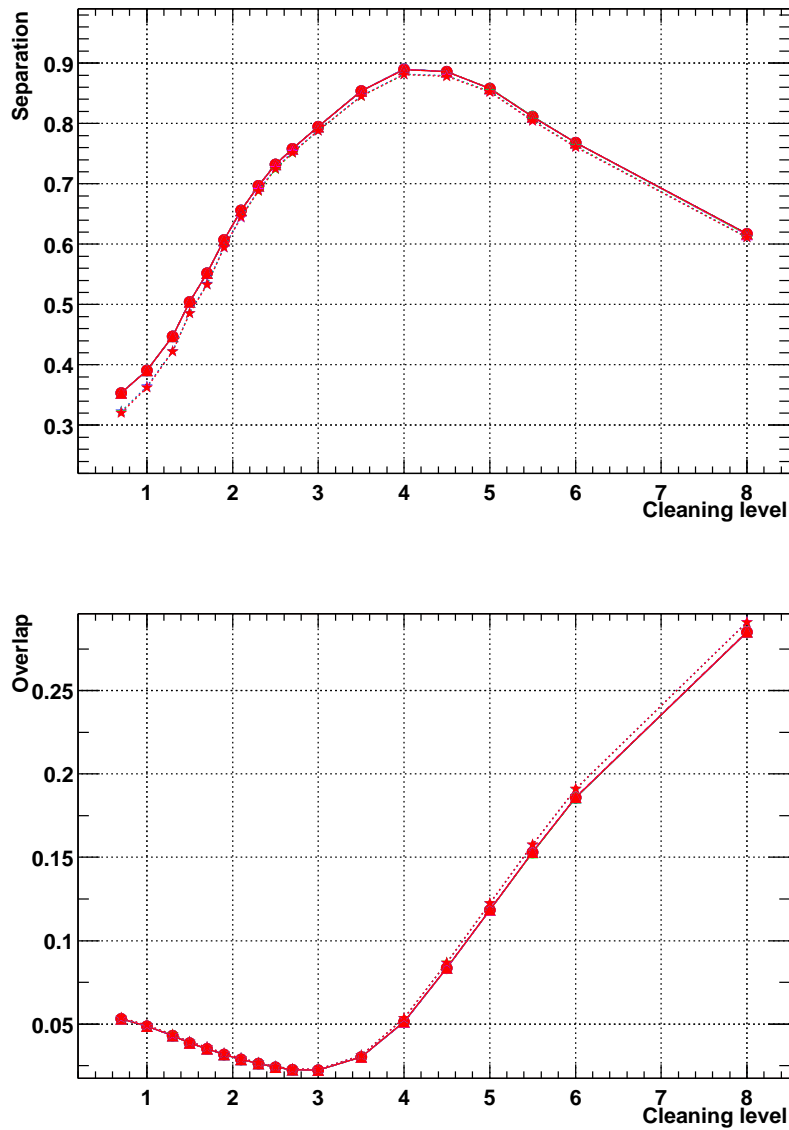


Figure A.25: The separation (above) and the overlap (below) for the parameter *Mountain-SIZE*. Optimal values for these two parameters are found for 'core' cleaning levels between **3 and 4**. The optimal values for the cleaning level for both parameters don't **coincide**, therefore the average of a level of **3.5** has been chosen.

Parameter	Cleaning level	Separation	Overlap
MultMountain	3.5/2.7	0.983	0.1083
MountainPhe	3.5/2.7	0.890	0.0512

Table A.4: The table presents the cleaning levels which provide the best separation and the smallest overlap. The cleaning level consists of two numbers. A 'core' limit and a 'border' limit.

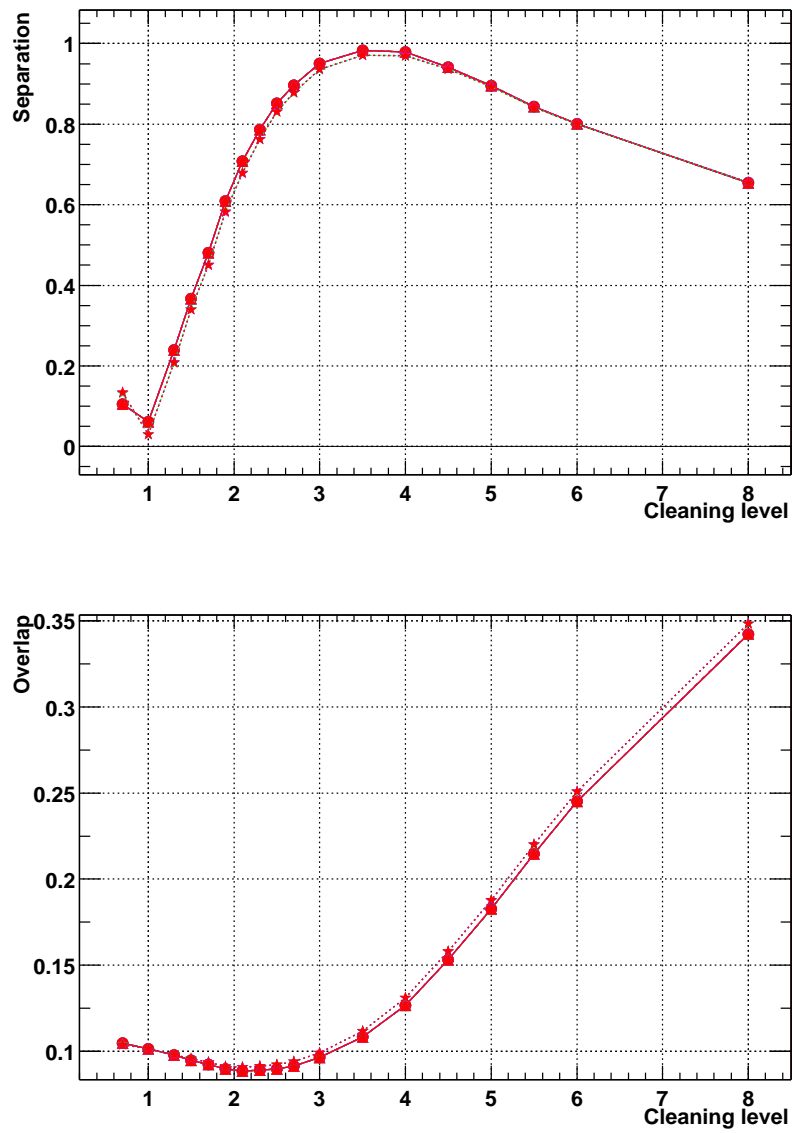


Figure A.26: The separation (above) and the overlap (below) for the parameter **Number-Mountain**. The parameters separation/overlap have optimal values for 'core' cleaning levels between **2 and 4**. They cleaning levels in the lower and upper plot . An intermediate value of a level of **3.5** was chosen.

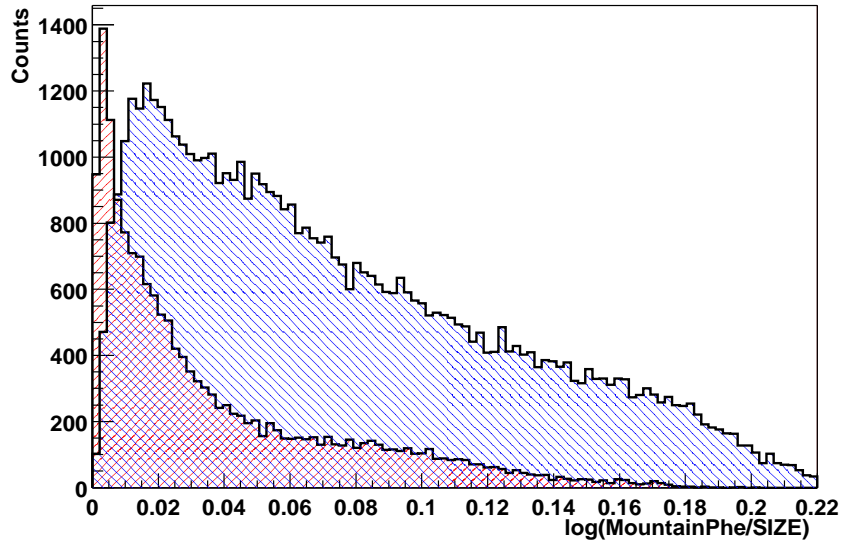


Figure A.27: Distribution of the Mountain-SIZE parameter, plotted as the logarithm of its ratio of Mountain-SIZE with SIZE for better illustration, for gammas (red) and for hadrons (blue). This distribution is not useful for hard cuts, but it improves the separation if used as a input in the LDA.

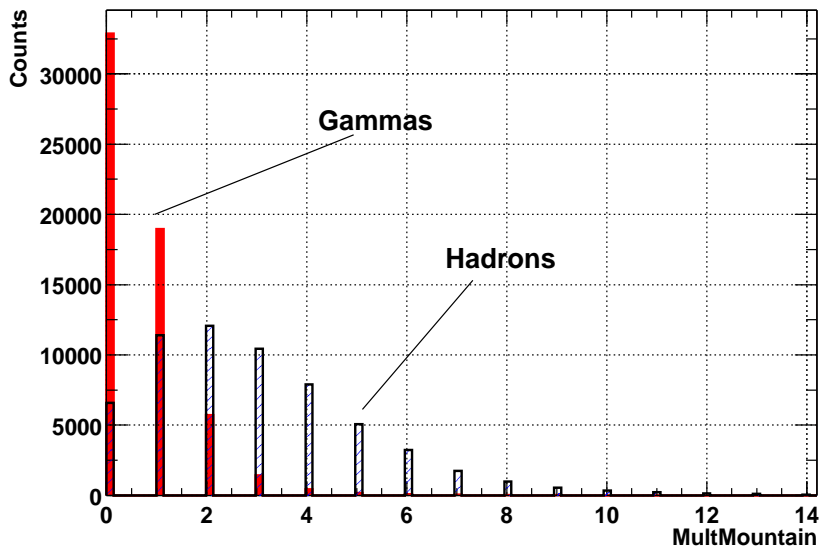


Figure A.28: Distribution of the Number-Mountain parameter for gammas (red) and for hadrons (blue). A hard cut on Number-Mountain  $< 2$  removes a sizable portion of the background while leaving most  $\gamma$ 's.